Received: 19 July 2013 ■ *Revised: 20 November 2013* ■ *Accepted: 11 December 2013* ■ *Publication: 21 January 2014*

JNIRS JOURNAL OF NEAR INFRARED SPECTROSCOPY

openaccess

Qualitative and quantitative pharmaceutical analysis with a novel hand-held miniature near infrared spectrometer

Manel Alcalà,[a*] Marcelo Blanco,[a] Daniel Moyano,[a] Neville W. Broad,[b] Nada O'Brien,[c] Don Friedrich,[c] Frank Pfeifer[d] and Heinz W. Siesler[d]

[a]Applied Chemometrics Research Group, Departament de Química, Facultat de Ciències, Universitat Autònoma de Barcelona, 08193 Bellaterra, Spain. E-mail: manel.alcala@uab.cat

[b]NWBSpectroscopy.co.uk, Laboratory G310, Building 110, Kent Science Park, Sittingbourne, Kent ME9 8AG, UK

[c]Optical Security and Performance Products, JDSU, Santa Rosa, CA 95407, USA

[d]Department of Physical Chemistry, University of Duisburg-Essen, 45117 Essen, Germany

Although miniaturisation of vibrational spectrometers began approximately a decade ago, only within the last couple of years have real hand-held Raman, infrared and near infrared (NIR) scanning spectrometers became commercially available. On the customer end the development of portable instrumentation was driven by the request for more flexibility of on-site measurements and on the manufacturer side it was supported by the potential and advantages of micro-electromechanical systems (MEMS) production and the implementation of new technologies. With reference to NIR spectroscopy the expectations for a real hand-held system (<100 g) have been recently realised by a pocket-sized spectrometer with a linear variable filter technology (LVF) as monochromator principle and the additional benefit of significantly reduced costs compared to other portable systems. For a real breakthrough and impact of this instrument, however, it had to be demonstrated that competitive analytical results can be achieved. In this respect, the present communication has put to test the performance of this micro-NIR system with reference to selected qualitative and quantitative pharmaceutical applications.

Keywords: hand-held NIR spectrometer, qualitative and quantitative pharmaceutical analysis, active ingredients, authentication, linear variable filter

Introduction

Over the last decade near infrared (NIR) spectroscopy has increasingly developed to become an indispensable analytical tool for production and quality control in the pharmaceutical industry.[1–4] Thus, qualitative NIR investigations are frequently applied for the identity control of incoming raw materials whereas quantitative analysis of the final product is an important step in the pharmaceutical process chain. However, the majority of pharmaceutical analyses are still performed by taking the sample in the production site and transporting it to the quality control laboratory that is located separately from the process. This delay between sampling and availability of results limits the frequency of analysis and the optimisation of the production line. Thus, novel portable field instrumentation capable of performing a rapid at-line or in-line analysis of the process can be considered as a key tool to advance the effectiveness of the pharmaceutical industry.[5]

This communication is intended to demonstrate the performance of a new portable micro-NIR spectrometer for the development of both qualitative and quantitative analytical methods of pharmaceutical raw materials, intermediates

ISSN: 0967-0335
doi: 10.1255/jnirs.1084

and final products. The selected case studies will cover the following topics accomplished by qualitative and quantitative investigations in combination with chemometric evaluation procedures.

Determination of counterfeit and illegal generic pharmaceuticals

The World Health Organization (WHO) estimates that roughly 10% of the world's pharmaceuticals may be counterfeit, and in parts of the developing world the rates are far higher. Illegal generic imports not only threaten public safety, but also erode a brand owner's profit margins. Counterfeiting and illegal drug imports are global crimes, with well-documented consequences.[6] With the rise in drugs purchased via the internet there follows the increase in illegal pharmacies pushing fake drugs or generic versions which are illegal in the country of export. An illegal generic can be perfectly legal in the country of origin, but typically not in the country of export destination. Portable, easy-to-use instrumentation able to perform rapid and non-destructive testing of the products is needed at border control and postal hubs in order to help identify such risks. A pocket-sized NIR spectrometer can satisfy this need whilst enabling the investigator to take on international travel as a carry-on luggage item and in some cases use inconspicuously in undercover investigation.

Though there has been research published on the use of NIR for discriminating counterfeit from authentic pharmaceutical products,[7–12] there has been less work dedicated to illegal generics analysis. One of the objectives of this work is to demonstrate the performance of the new miniaturised NIR spectrometer based on a qualitative study, whereby the discrimination between illegal generic and authentic pharmaceutical products is successfully accomplished.

Development of a spectral library for raw material identification

The identification of raw materials used to manufacture products is one of the routine tests used to control pharmaceutical processes. The identification verifies the identity of a given substance. The need for this identification test is acknowledged in various International Conference on Harmonisation of Technical Requirements for Registration of Pharmaceuticals for Human Use (ICH) guidelines for pharmaceuticals. The construction of NIR libraries containing the spectra for all the compounds potentially handled by a pharmaceutical manufacturer avoids the need to develop a specific method for each and allows the compounds to be identified by using a single, straightforward, expeditious, inexpensive method.[13]

Quantitative determination of active ingredients in solid pharmaceutical formulations

Blending of powder formulations during a pharmaceutical production process is important to obtain homogeneous mixtures before tablet compaction. The unit dose uniformity depends basically on the correct distribution of active principle ingredient (API) within the batch.[14] Spectroscopic measurements with the micro-NIR spectrometer as part of this communication have provided the necessary data basis to develop quantitative calibration models for the determination of API concentration at the end of a blending operation.

Instrumentation

The MicroNIR™ spectrometer is a new instrument developed and commercialised by JDSU Corporation (Santa Rosa, CA, USA). It is designed to measure diffuse reflectance in the NIR region of the electromagnetic spectrum. The MicroNIR owes its small size to the novel thin-film linear variable filter (LVF) used as the dispersive element. The LVF is a dielectric thin-film Fabry–Perot bandpass filter deposited using energetic processes, well-known to produce stable and reliable optical components.[15] The filter coating in the LVF is intentionally wedged in one direction. Since the centre wavelength of the bandpass filter is a function of the coating thickness, the peak transmitted wavelength varies continuously along the direction of the wedge. This working principle is illustrated in Figure 1. The LVF component can be compared to a scanning Fabry–Perot interferometer that scans with position instead of time.

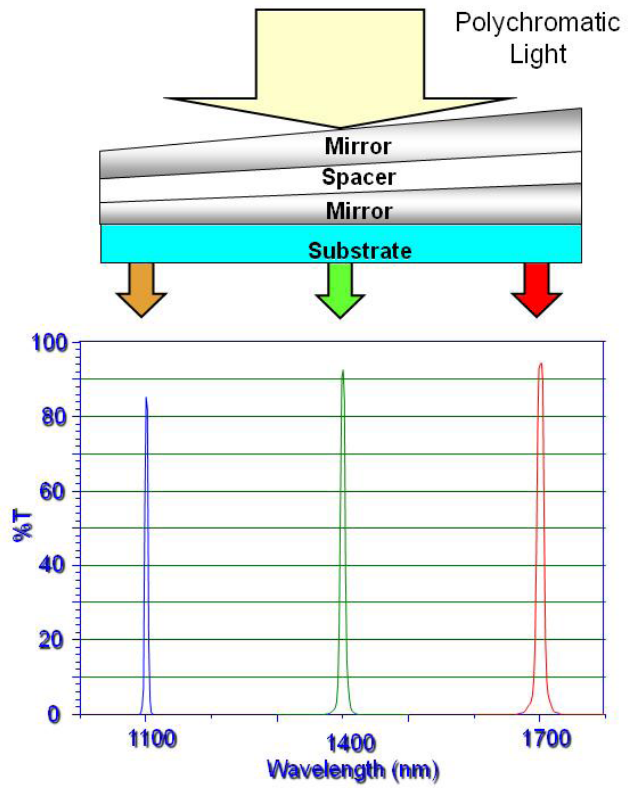

Figure 1. Working principle of a linear variable filter (NIR) component. The wedge in the thickness is applied to all layers comprising the bandpass filter design.

Figure 2. The MicroNIR spectrometer.

The MicroNIR employs an LVF component directly bonded to a linear detector array, which results in an extremely compact and rugged spectral engine with no moving parts. The LVF makes each pixel of the detector respond to a different wavelength. This ultra-compact spectroscopic engine is coupled with miniaturised readout electronics and a tungsten lamp diffuse illumination system. The entire unit is USB-powered and scarcely larger than a golf ball. An image of the MicroNIR spectrometer is provided in Figure 2.

Figure 3 shows a schematic illustration of MicroNIR's optical design. In the diffuse reflection mode, shown in Figure 3(a), two built-in tungsten lamps flood-illuminate a spot on the sample under test that is approximately 3 mm in diameter, at a 3 mm distance from the instrument. The diffusely reflected radiation is collected and delivered to the spectral engine, which is read by the electronics and displayed on a computer. Although the optimal working distance is approximately 3 mm, longer working distances are also possible, which can be useful for transflection applications (viewing a white standard through a sample liquid, for example). Figure 3(b) shows the MicroNIR in a transmission configuration. An external lamp illuminates a cuvette with collimated light, and the MicroNIR is used with lamps off to measure the transmission. Figure

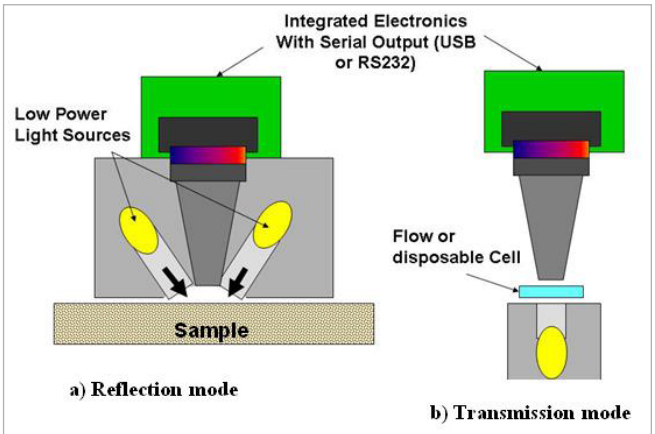

Figure 3. A schematic illustration of the optical design of a JDSU MicroNIR spectrometer in the (a) diffuse reflection mode and (b) transmission mode.

Figure 4. Measurement set-ups in reflection mode and sample presentation for the investigation. On the left, the lamps are pointing up and the 100% reflectance reference is placed inside a glass cuvette. On the right, the lamps are pointing down directly over the sample surface.

4 shows two examples of measurement set-ups in reflection mode that have been used for this investigation. On the left, the lamps are pointing up and the sample is placed inside a glass cuvette. On the right, the lamps are pointing down over the sample surface. Depending on the absorbing properties of the glass cuvette, the reference can be acquired placing the 100% reflectance inside the cuvette and measuring through the glass of or without the cuvette.

Key attributes of the two MicroNIR spectrometer versions are summarised in Table 1. Both MicroNIR's were used for the studies in this paper. The extended version was tailored to monitor the wavelength range of an indium gallium arsenide (InGaAs) detector, covering the 1150–2150 nm (8695–4651 cm^{-1}) range. The standard InGaAs detector wavelength range is another common option of the MicroNIR covering the 950–1650 nm (10,526–6060 cm^{-1}) range. Other custom wavelength ranges are possible.

Discussion of the qualitative and quantitative applications

Determination of counterfeit and illegal generic pharmaceuticals

Materials and methods

Samples

Various authentic, counterfeit and illegal generic pharmaceutical products were analysed using the standard version of the MicroNIR (1700) spectrometer. Two types of pharmaceutical products were evaluated: weight loss and erectile dysfunction (ED) treatment products. The weight loss product was GSK Alli® 60 mg (Orlistat) capsules and a counterfeit version of the product. The ED products were Pfizer's Viagra (Sildenafil Citrate), Cialis (Tadalafil) and several illegal generic versions. The investigated samples are listed in Table 2. In all, three

Table 1. Key performance attributes of the JDSU MicroNIR spectrometer.

Weight	60 g
Dimensions	45 mm diameter × 42 mm height
Spectral range	Extended: 1150–2150 nm; Standard: 950–1650 nm
Optical resolution	<1.25% of centre wavelength, i.e. at 1000 nm wavelength, resolution is <12.5 nm; at 2000 nm, <25 nm resolution
Geometric resolution	Extended: 8 nm per pixel; Standard: 6.25 nm per pixel
Power requirement	USB powered, <500 mA at 5V
Operating temperature	–20°C to 40°C

Table 2. Investigated authentic, counterfeit or illegal generic samples.

Authentic sample	Sample identifier	Type	Counterfeit or illegal generic sample (comparator)	Sample identifier	Type
Alli® 60 mg	Alli_1 to 3	Authentic slimming tablet	CF-Alli (Sibutramine)	CFAlli_1 to 3	Counterfeit slimming pill (Sibutramine)
Viagra® 25 mg	Sil25_1 to 3	Authentic Viagra® 25 mg	Kamagra 100 mg	IG_A_1 to 3	Illegal generic (A) Sildenafil 100 mg
Viagra® 50 mg	Sil50_1 to 3	Authentic Viagra® 50 mg	Zenegra 100 mg	IG_B_1 to 3	Illegal generic (B) Sildenafil 100 mg
Viagra® 100 mg	Sil100_1 to 3	Authentic Viagra® 100 mg	Sildigra XL 150 mg	IG_C_1 to 3	Illegal generic (C) Sildenafil 150 mg
Cialis® 2.5 mg	Tad2_5_1 to 3	Authentic Cialis® 2.5 mg	—	—	—
Cialis® 5 mg	Tad5_1 to 3	Authentic Cialis® 5 mg	—	—	—
Cialis® 10 mg	Tad10_1 to 3	Authentic Cialis® 10 mg	Tadfil 20 mg	IG_D_1 to 3	Illegal generic (D) Tadalafil 20 mg
Cialis® 20 mg	Tad20_1 to 3	Authentic Cialis® 20 mg	Tadora 20 mg	IG_E_1 to 3	Illegal generic (E) Tadalafil 20 mg

types of illegal generic Sildenafil tablets were tested and labeled as IG_ (Illegal Generic) A, B and C, and two illegal generic versions of Tadalafil, labeled IG_E and F. A counterfeit version of Alli® was also analysed.

Experimental

Prior to sample analysis, the MicroNIR wavelength scale was verified using a USP NIR wavelength standard (Lot F0G007, Catalogue number 1457844). The NIR spectrometer was zeroed (0% reflectance) using a 2% reflective dark reference (from LabSphere) and a 100% baseline then achieved measuring a 99% reflective Spectralon™ ceramic reference (also from LabSphere). This sequence of re-zeroing and baseline acquisition was repeated once every 15 min during sample analysis periods.

All samples were measured by placing them over the sapphire window of the MicroNIR spectrometer. The content of the capsules were emptied into glass vials and measured through the bottom of the vial. The tablets were measured as is.

Capsule Analysis: Powder blends in vials were each measured three times, inverting and re-presenting the blend each time, to give maximum analysis variance.

Tablet Analysis: Three tablets were measured for each sample brand. Tablets of the same brand were scanned in exactly the same orientation to minimise stray light and reflectance differences. Each of the three tablets was then measured once, with the brand owner's logo face downwards (towards the lamps) and the strength numeration is facing up (away from lamps). 60 scans were taken per sample spectrum, with an integration time of 5600 µs. Each spectrum was the mean of 60 scans in the wavelength range 880–1168 nm at 6 nm data point intervals.

Data analysis

For authentic, counterfeits and illegal generic comparisons, second derivative absorbance (Savitzky–Golay, 11 data points, 2nd order polynomial) was achieved by exporting the MicroNIR's IRSE-XP software reflectance data into the Unscrambler GENX

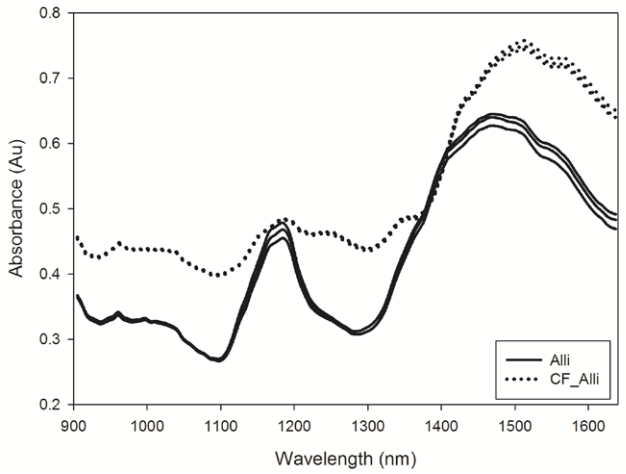

Figure 5. Absorbance NIR spectra of the authentic and counterfeit (CF) Alli® capsule blends.

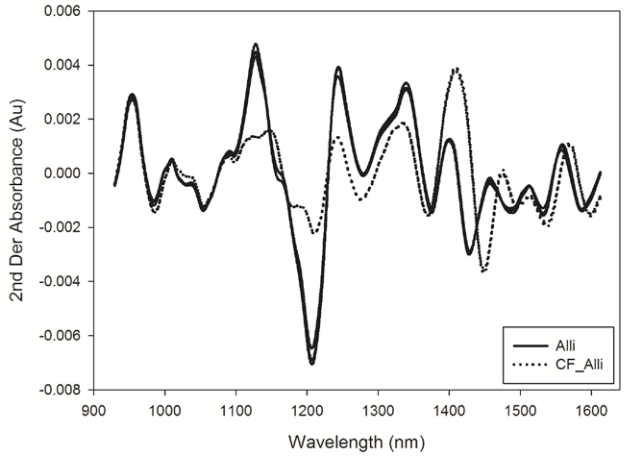

Figure 6. Second derivative absorbance NIR spectra of the authentic and counterfeit Alli® capsule blends.

v. 10.2. First, a transpose of the spectral data from reflectance to absorbance was made, then a second derivative transformation of the absorbance data was performed. Authentic ED tablets were distinguished from illegal generics by exporting the second derivative absorbance data into software for the generation of principal components analysis (PCA). The chemometric software used was Unscrambler GENX v. 10.2 (Camo A/S Software, Norway). Finally, Microsoft Excel® (2010 Edition) was programmed to generate 95% equal frequency ellipse plots.[12]

Results and discussion

Authentic and counterfeit Alli® (Orlistat) capsule blends

The significance of the data, and hence review of the instrument suitability for this application, was achieved by comparison of the authentic product with the counterfeit and/or illegal generic product.

Figure 5 shows the absorbance spectra of Alli® 60 mg and the counterfeit "CF_Alli". Distinct differences can be clearly seen. Differences, however, are more easily seen with second-derivative spectra (Savitzky–Golay, nine data points, 2nd order polynomial smoothing) in the region 1435 nm of Figure 6. Using this simple second derivative approach, it is possible to distinguish between genuine and counterfeit slimming capsules with little sample preparation and rapid analysis time. The counterfeit samples contained Sibutramine, and not Orlistat.

Authentic and illegal generic Sildenafil tablets

Principal component analysis provides a more powerful method of distinguishing between samples. PCA was performed on the second derivative absorbance data from each authentic Viagra® strength (25 mg, 50 mg and 100 mg Sildenafil) and the illegal generic Kamagra 100 mg (IG_A), Zenegra 100 mg (IG_B) and Sildigra XL 150 mg (IG_C) tablets. Figure 7 shows the PCA scores plot for each authentic Sildenafil strength and illegal generic. The first principal component explains 66% of the second derivative spectral variability, and discriminates the authentic from the illegal generic Sildenafil tablets. As all the authentic Viagra® tablets have the same coating, and are compressed from a common blend, it is, therefore not surprising that there is no particular separation of authentic tablet strength using the MicroNIR spectrometer.

In the same Figure 7 the data is calculated with a 95% equal frequency ellipse around the authentic tablets (all strengths group together) and plots the scores points for the Kamagra 100 mg, (IG_A), Zenegra 100 mg (IG_B) and Sildigra XL 150 mg (IG_C) tablet sets. Any individual tablet (illegal generic or otherwise) that falls outside the 95% equal frequency ellipse is highly unlikely to come from the same source. The authentic

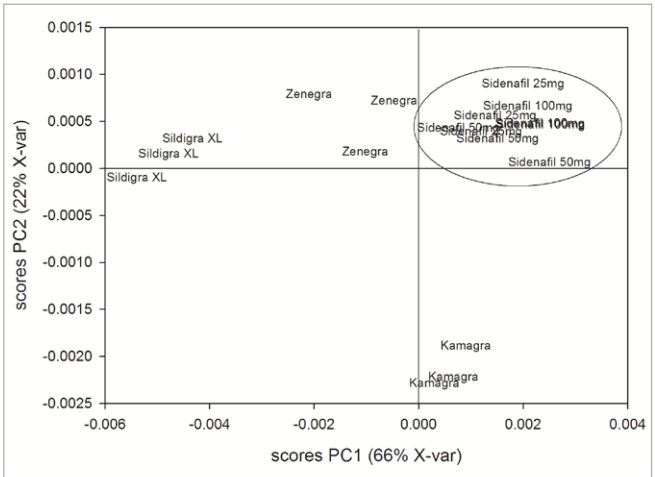

Figure 7. Principal component analysis (PCA) scores plot of the first and second PC obtained from the NIR spectra of authentic strengths and illegal generic Sildenafil types in 2nd derivative mode, with authentic Sildenafil strengths shown, showing an equal frequency ellipse for authentic Sildenafil at a 95% confidence limit.

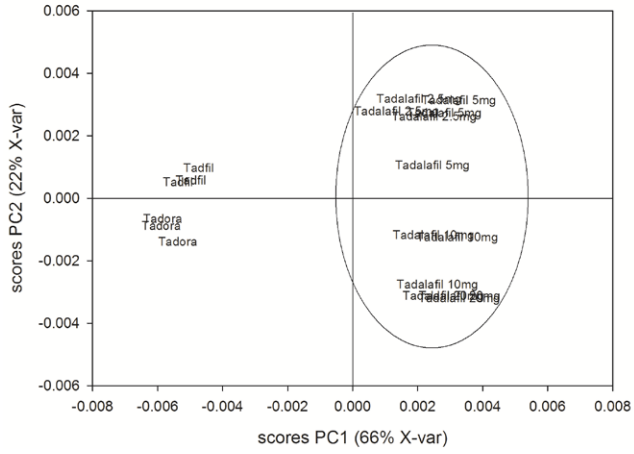

Figure 8. Principal component analysis (PCA) scores plot of the first and second PC obtained from the NIR spectra of authentic strengths and illegal generic Tadalafil types in 2nd derivative mode, with authentic Tadalafil strengths shown, showing an equal frequency ellipse for authentic Tadalafil at a 95% confidence limit.

tablets were discriminated from the illegal generic types, with Zenegra 100 mg being most similar in NIR spectra and therefore organic composition to the Pfizer product. Kamagra was discriminated from all other products along the second PC.

Authentic and illegal generic Tadalafil tablets

PCA was performed on the second derivative absorbance data for each of the different authentic Cialis® strengths (Tadalafil 2.5 mg, 5 mg, 10 mg and 20 mg) and the illegal generic Tadfil 20 mg (IG_D), and Tadora 20 mg (IG_E) tablets. Figure 8 shows the PCA scores plot for each authentic Tadalafil strength and the illegal generic.

The first principal component (66% variance explained) separated the authentic from the illegal generic Tadalafil types. It is interesting to note that the PC2 (22%) separated the illegal generic brands, and also in the case of the authentic tablets, the smaller 2.5 mg and 5 mg tablets were distinguished from the larger 10 mg and 20 mg Cialis®.

Figure 8 also shows the same data with an equal frequency ellipse for authentic Tadalafil at a 95% confidence limit. The illegal generic tablets were extremely dissimilar to the authentic types using the MicroNIR technology.

Development of spectral library for raw material identification

Materials and methods

Samples

The spectral library includes 24 different raw materials that include: Citric Acid, Anhydrous (Citrique Belge S.A., Tienen, Belgium), Starch maize (Cargill Benelux, La Sas van Gent, Netherlands), Beclometasone Dipropionate (Crystal Pharma, Valladolid, Spain), Carbomer (3V Sigma SpA, Bergamo, Italy), Cellulose Microcrystalline 50 µm (JRS Pharma, Weissenborn, Germany), Deflazacort (Sanofi Aventis, Brindisi, Italy), Dexketoprofen and Dexketoprofen Trometamol (Lusochimica SpA, Pisa, Italy), Glycerol Distearate type I (Gattefosse SAS, Sant Priest, France), Fructose (Danisco Sweeteners SA, Kotka, Finland), Gemfibrozil (Hikal Limited, Karnataba State, India), Lactose Monohydrate (Meggle, Wasserburg, Germany), Macrogol Cetostearyl Ether 22 (Croda Ibérica SA, Fogars de la Selva, Spain), Maltodextrin (Roquette Freres, Lestrem, France), Mannitol and Mannitol granulate (Roquette Freres, Lestrem, France), Sorbitan Monostearate (Croda Ibérica SA, Fogars de la Selva, Spain), Nimesulide (Aarti Drugs Ltd, Maharashtra, India), Otilonium Bromide (Sifavitor Srl, Casaletto Lodigiano, Italy), Sucrose crystal and sucrose powder (Tereos, Bucy le Long, France), Triflusal (Urquima SA Uriach Group, Sant Fost de Campsentelles, Spain).

Experimental

The powder sample is placed inside a glass cuvette on the window of the MicroNIR where the light sources and detector are placed. A white 99% reflectance ceramic reference is placed inside an empty glass cuvette before the spectral acquisition of a sample. The spectrum of a sample is obtained from the average of three spectra.

Data analysis

The chemometric software used for the spectral pretreatment and the calculation of the cross-correlation tables was Unscrambler v. 9.8 (Camo Software, Norway). Changes in software version regard to user-friendliness functions and certainly not to algorithms. There is no reason to expect any changes in the results regarding the statistical parameters.

Results and discussion

Typically, unsupervised pattern recognition methods such as correlation coefficient in the wavelength space can be used for the identification of an unknown sample. The development of a spectral library for pharmaceutical raw material identification needs, at least, three different batches of each compound. However, only two batches for each of 23 different raw materials were available for this study. The authors decided to use one batch of each compound to include on every calibration class and the other one to evaluate the identification predictive ability of the spectral library. It is understood that this number of samples is not enough to calculate a spectral library for routine analysis, but this was not the scope of the study. The number of available samples is enough to evaluate the feasibility of using the MicroNIR unit for raw material identification.

Different smoothing pretreatments of the spectra (moving average, median filter and Gaussian filter) were tested followed by second derivative (gap-segment and Norris gap). There are three main aspects to be evaluated during the calculation of the spectral library. First, the correlation between the spectra of two different raw materials should be lower than the predefined threshold of 0.97. Second, the correlation between the calibration and prediction spectra of the same raw material should be higher than the threshold (positive identification).

Table 3. Correlation coefficient for the identification of 22 raw materials. Threshold for positive identification is $r > 0.97$.

Raw material	Correlation coefficient (r)
Citric acid	0.992
Maize starch	0.999
Beclomethasone dipropionate	0.996
Carbomer	0.977
Microcrystalline cellulose	0.996
Deflazacort	0.993
Dexketoprofen trometamol	0.995
Dexketoprofen	0.998
Fructose	0.999
Gemfibrozil	0.977
Glycerol distearate	0.992
Lactose monohydrate	1.000
Macrogol cetostearyl ether	0.997
Maltodextrin	0.987
Mannitol granulate	0.999
Mannitol	1.000
Sorbitan monostearate	0.999
Nimesulide	0.996
Otilonium bromide	1.000
Sucrose powder	0.991
Sucrose crystal	0.987
Triflusal	0.998

Third, the correlation between the calibration spectrum of one material and the prediction spectrum of another material should be lower than the threshold (false positive). The objective is to select the most appropriate spectral pretreatment combination to positively reach the three aspects.

The combination of spectral pretreatment that allows the better identification performance is a moving average smoothing (segment of three) followed by a gap-segment second derivative (three and three segments). Table 3 shows the correlation coefficient calculated between the spectra of the calibration and prediction for each individual raw material. As can be seen, all the coefficients are higher than the threshold of 0.97 which means positive identifications for each compound.

Table 4 shows the correlation coefficient for the false positive identifications. This means that raw material 1 is wrongly identified as raw material 2, because of the high spectral similarity between the two compounds. The higher correlation is obtained for the pair mannitol–mannitol granules ($r = 0.995$). The unique difference between them is the particle size (fine powder and granules). The second derivative spectral pretreatment reduces the additive and multiplicative scattering effects of the radiation that are mainly promoted by the differences on particle size. After the spectral pretreatment, the spectra of the two mannitols are virtually the same, so it is not possible to differentiate between them using the correlation coefficient based on the wavelength space. The use of a pattern recognition method based on the principal component space solves this problem. It is strictly necessary to have a higher number of different batches to calculate the qualification sub-library. As mentioned before, the available number of samples is not sufficient to perform this calculation. Following Table 4, the second higher correlation is obtained for the pair sucrose powder–sucrose crystal ($r = 0.982$), that is a very similar case to the mannitols. Both sucroses presented differences in the particle size distribution. Table 4 also includes another two examples that correspond to the third and fourth higher correlations. Even though the obtained values are lower than the threshold of $r = 0.97$, it is important to mention that the larger similarity of chemical structure between two different materials, the higher spectral correlation will be obtained. This is the case for the pairs glycerol distearate–sorbitan monostearate ($r = 0.957$) and maize starch–maltodextrin ($r = 0.954$). In this spectral library there are no false positive identifications for these two last pairs, as the calculated correlations are lower than the threshold 0.97, but it would be interesting to evaluate them with a larger number of samples. Eventually, qualification sub-libraries based on PCA would be needed to solve the cross-identifications around the threshold.

Table 4. False positive and near-false positive identifications.

Raw material 1	Raw material 2	Correlation coefficient (r)
Mannitol	Mannitol granulate	0.995
Sucrose powder	Sucrose crystal	0.982
Glycerol distearate	Sorbitan monostearate	0.957
Maize starch	Maltodextrin	0.954

Quantitative determination of active ingredients in solid pharmaceutical formulations

Determination of three active ingredients in a five-component pharmaceutical powder formulation

Samples and experimental

The investigated solid drug formulations consisted of mixtures of the three crystalline active ingredients acetylsalicylic acid ASA (Sigma-Aldrich Chemie GmbH, Steinheim, Germany), ascorbic acid ASC (Acros Organics, New Jersey, USA) and caffeine CAF (Sigma-Aldrich Chemie GmbH, Steinheim, Germany) with the two amorphous excipients cellulose CE (Fluka Chemie GmbH, Buchs, Switzerland) and starch ST (Carl Roth GmbH, Karlsruhe, Germany).

A set of 48 samples was prepared by milling varying amounts of the three active ingredients in the concentration range 13.77–26.43% (w/w) with equal amounts [40% (w/w)]

Table 5. Chemical composition of the investigated pharmaceutical formulations.

	Max % (w/w)	Min % (w/w)	Σ % (w/w)
ASA	26.04	15.22	60
ASC	26.19	14.77	
CF	26.43	13.77	
CE/ST (1:3)	40	40	40

of a 1:3 (w/w) mixture of cellulose and starch (Table 5 and 6) for 5 min in a Retsch mill (type BMO, Retsch GmbH, Haan, Germany). The final particle size of the mixtures after the milling procedure varied between about 10 µm and 30 µm (Figure 9).

For the diffuse reflection measurements the extended version of the MicroNIR (2200) system was applied and the powder samples were presented in a small brass cup positioned under the spectrometer (Figure 4). Each sample was measured in the temperature range 22–24°C in triplicate by re-pack of the brass cup and the reference spectra

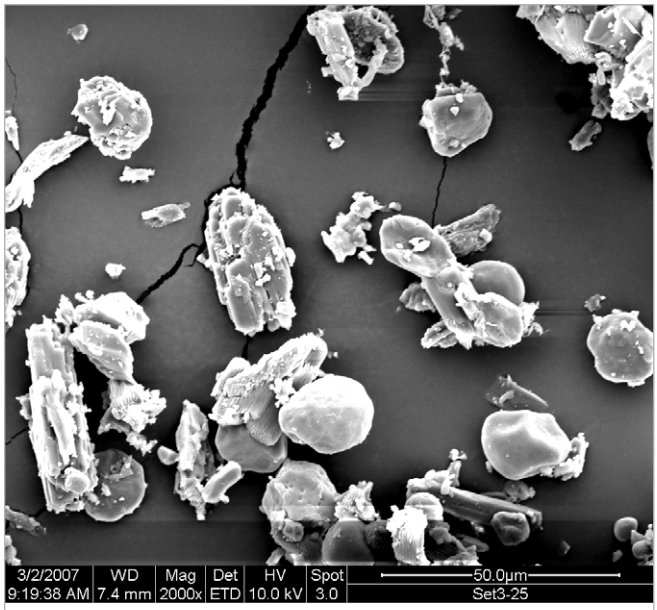

Figure 9. Scanning electron micrograph of a typical drug formulation.

Table 6. Composition of the 48 investigated pharmaceutical formulations (22, 24, 38: test samples).

No.	ASA % (w/w)	ASC % (w/w)	CF % (w/w)	CE:ST (1:3), % (w/w)
1	21.78	20.46	17.68	40
2	19.25	18.11	22.64	40
3	17.3	16.27	26.43	40
4	20.54	22.55	16.91	40
5	18.32	20.13	21.55	40
6	17.05	18.71	23.03	40
7	19.11	23.97	17.7	40
8	17.21	21.59	21.85	40
9	15.85	19.88	24.27	40
10	18.55	26.19	15.25	40
11	16.73	23.6	19.67	40
12	15.22	21.48	23.29	40
13	23.27	19.58	17.15	40
14	20.73	17.44	21.83	40
15	18.69	15.73	25.58	40
16	22.07	21.67	16.26	40
17	19.77	19.42	20.81	40
18	17.91	17.59	24.5	40
19	20.99	23.55	15.46	40
20	18.89	21.21	19.91	40
21	17.19	19.29	23.53	40
22	20.01	25.26	14.73	40
23	18.1	22.85	19.05	40
24	16.52	20.87	22.61	40
25	24.72	18.83	16.45	40
26	22.11	16.85	21.05	40
27	20.01	15.24	24.76	40
28	23.48	20.86	15.67	40
29	21.11	18.77	20.13	40
30	19.19	17.04	23.76	40
31	22.37	22.74	14.88	40
32	20.22	20.53	19.25	40
33	18.45	18.74	22.81	40
34	21.35	24.41	14.24	40
35	19.4	22.15	18.46	40
36	17.75	20.28	21.97	40
37	26.04	18.11	15.85	40
38	23.39	16.27	20.34	40
39	21.23	14.77	24	40
40	24.79	20.13	15.08	40
41	22.38	18.16	19.47	40
42	20.4	16.55	23.06	40
43	23.66	21.95	14.39	40
44	21.45	19.89	18.66	40
45	19.64	18.21	22.15	40
46	22.63	23.6	13.77	40
47	20.59	21.5	17.91	40
48	18.91	19.74	21.35	40

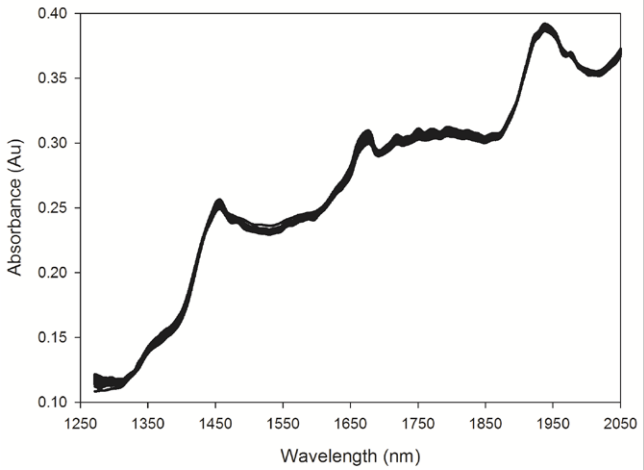

Figure 10. EMSC pretreated mean spectra of three replicate measurements of the pharmaceutical formulations recorded with the MicroNIR 2200 spectrometer in the calibration wavelength range (1271–2051 nm).

were acquired with the 99% R reflectance standard after every three replicate measurements of each sample. The measurement parameters were configured to an integration time of 1000 µs and a scan number of 10,000. The original spectra were recorded in the 9025–4673 cm^{-1} wavenumber region.

Chemometric data evaluation

The data pretreatment, development of the cross-validated PLS-1 calibration models for the formulation components (ASA, ASC and CF) and the prediction of the independent test samples were performed with the Unscrambler™ software (version 9.6; CAMO Software AS, Oslo, Norway). After calculating the mean spectra of the replicate measurements for each sample and visual inspection of the original data set, only the 7866–4875 cm^{-1} range was selected and an extended multiplicative scatter correction (EMSC) was applied before the development of PLS-1 calibration models for the active ingredients (Figure 10).

Results and discussion

In Table 7 the actual/prediction figures of merit of the calibration/cross validation parameters for the three active ingredients are summarised. The prediction of the test samples which had been carefully selected in terms of the compositional variance of their active ingredients are summarised in Table 8. Good agreements between the reference values and the predicted values of the test samples have been obtained which is competitive with results previously obtained with a benchtop and other portable systems.[16]

Determination of active principle ingredient in a powder pharmaceutical sample

Samples and experimental

The pharmaceutical formulation analysed by the quantitative method contains Cetirizine Dihydrochloride (Arch Pharmalabs, Maharashtra, India) as the unique active principal ingredient (API 9% w/w), Cellulose Microcrystalline 90 µm (FMC Biopolymer International, Cork, Ireland) and Lactose Monohydrate (Meggle, Wasserburg, Germany) as major excipients (90% w/w), Magnesium Stearate (Peter Greven, Münstereifel, Germany) and Silica Colloidal Anhydrous (Wacker Chemie AG, Burghausen, Germany) as minor excipients (1% w/w). Twenty-four different samples were prepared in the laboratory. Appropriate amounts of API and excipients were weighed with an analytical balance and mixed. The total amount per sample was approximately 10 g. This laboratory sample set encompassed a ±20% relative concentration range around the target value for the API and ±5% for all the excipients. The API concentration range was approximately 7.0–10.5% w/w. Each concentration level for every sample was selected using an appropriate D-optimal design that reduced the cross-correlation between the concentrations of all the components of the formulation. This strategy of sample preparation improves the predictive ability of the multivariate

Table 7. PLS 1 calibration/cross validation parameters for the three active ingredients [a: ASA (three outliers, four factors); b: ASC (one outlier, six factors); c: CF (three outliers, six factors)] after EMSC pretreatment.

	Number of samples	Slope	Offset	Correlation	*RMSEC* % (w/w)	*SEC* % (w/w)	Bias % (w/w)
ASA							
Calibration	42	0.967	0.665	0.983	0.454	0.460	0.000
Cross-validation	42	0.931	1.381	0.972	0.582	0.589	–0.003
ASC							
Calibration	44	0.974	0.524	0.987	0.422	0.427	0.000
Cross-validation	44	0.945	1.010	0.961	0.722	0.731	0.003
CF							
Calibration	42	0.978	0.440	0.989	0.522	0.528	0.000
Cross-validation	42	0.951	0.975	0.969	0.857	0.867	0.007

Table 8. Prediction of the ASA, ASC and CF content % (w/w) of the three test set samples based on the PLS 1 calibration models detailed in Figure 14.

ASA	% (w/w)	
Sample	**Predicted**	**Reference**
Pharma22_M	21.11	20.01
Pharma24_M	15.97	16.52
Pharma38_M	23.43	23.39
ASC	**% w/w**	
Sample	**Predicted**	**Reference**
Pharma22_M	25.82	25.26
Pharma24_M	21.45	20.87
Pharma38_M	16.14	16.27
CF	**% w/w**	
Sample	**Predicted**	**Reference**
Pharma22_M	14.02	14.73
Pharma24_M	22.09	22.61
Pharma38_M	19.92	20.34

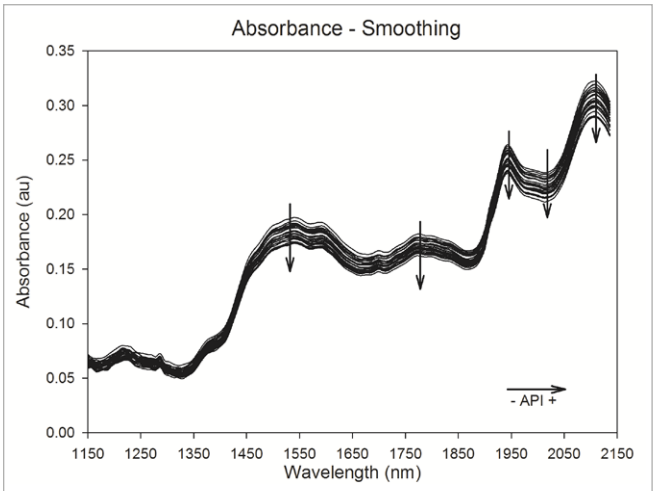

Figure 11. Absorbance NIR spectra of the laboratory sample set encompassing an API concentration range between 7.2% and 10.8% (w/w).

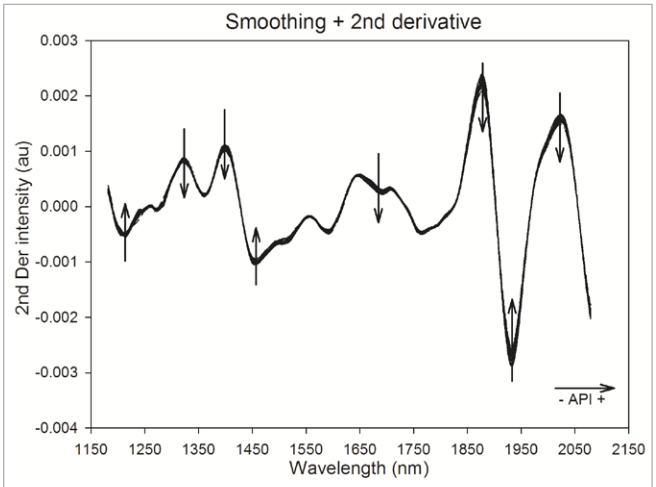

Figure 12. Second derivative NIR spectra of the laboratory sample set encompassing an API concentration range between 7.2% and 10.8% (w/w).

calibration model for API quantification. Beside this laboratory 24-sample set, two industrial samples were withdrawn at the end of the blending operation of the manufacturing process.

Chemometric data evaluation

The chemometric software used for the spectral pretreatment and the calibration models was Unscrambler v. 9.8 (Camo Software, Norway). Partial Least Squares (PLS) calibration models were calculated by cross-validation, using the leave-one-out method. The quality of the models was assessed in terms of the root mean square error of calibration (%*RMSEC*) and prediction (%*RMSEP*) defined as

$$RMSE(\%) = \sqrt{\frac{\sum_{i=1}^{n}(Y_i^{pred} - Y_i^{ref})^2}{n}} \quad (1)$$

where n is the number of samples used, Y^{ref} the concentration provided by the reference method and Y^{pred} that estimated by the NIR method. The number of PLS factors required to define the model was chosen from the minimum of a plot of *RMSEP* vs number of factors.

Results and discussion

Blending operations of raw materials before tablet compaction must ensure that homogeneous blends are obtained. It is important to develop analytical methods for the prediction of the API concentration in the blends at this point. An API concentration value within specifications is essential before proceeding with subsequent manufacturing operations.

Figures 11 and 12 shows the Absorbance and 2nd derivative NIR spectra, respectively, of the laboratory sample set encompassing an API concentration range between 7.2% and 10.8% w/w. As can be seen, there are a number of bands where the intensity changes accordingly with the different API concentration. Principal component analysis (PCA) was applied to the 2nd derivative NIR spectra of the laboratory sample set. Figure 13 represents the scores plot of PC1 vs PC2. The scores distribution along the PC1 axis (80% X-variance) followed the concentration values, demonstrating the spectral sensitivity of the spectrometer for this sample set. The scores plot of the PCA was used to split the sample set in two subsets, namely calibration (17 samples) and validation (7 samples).

The objective of this part of the study includes the development of a quantitative method for the determination of the API concentration of an industrial powder pharmaceutical blend. Partial least squares multivariate calibration models were calculated using only laboratory samples that mimic the production samples. A number of different combinations of

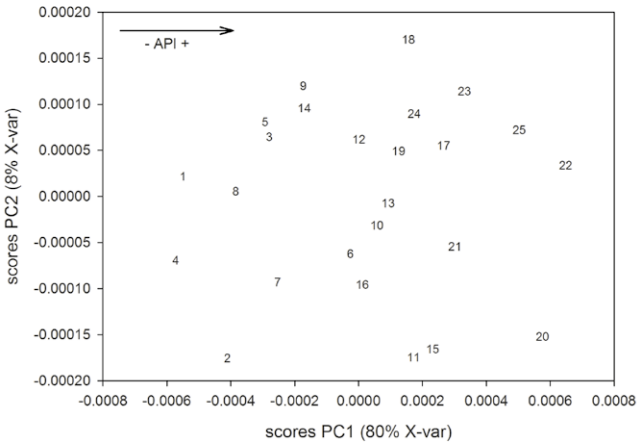

Figure 13. Principal component analysis (PCA) scores plot of the first and second PC obtained from the NIR spectra of laboratory sample set in 2nd derivative mode. Scores symbols represented as sample identification numbers from 1 to 22 (lowest to highest concentration).

spectral pretreatments were tested to evaluate the calibration performance and the predictive ability of the PLS models (smoothing of moving average, median filter and Gaussian filter, SNV and first and second derivatives of gap-segment and Norris gap). Table 9 shows a summary of the most relevant models that were calculated. The minimum number of factors to reach a calibration correlation of 0.99 and a minimum of 95% *Y*-explained variance is between four and five. For all the cases, the Root Mean Square Error of Calibration (*RMSEC* % w/w) is between 0.091 and 0.172 which is considered as a good calibration performance for all the PLS models. However, only the two last PLS models (2nd Derivative without/with smoothing) reveals good predictive ability (*RMSEP* % w/w of 0.2 and correlation of 0.98). The validation statistics for these two PLS models using four factors are virtually identical and the predictive ability for laboratory samples is demonstrated through the residual Student t-test (t-calculated value lower than t-critical, 95% significance).

The PLS models that demonstrated the best predictive ability for laboratory samples were used to calculate the API concentration of the two industrial samples. The predictive ability of the model calculated with the spectral pretreatment of smoothing Gaussian filter (segment of three) followed by 2nd derivative gap–segment (three–three) was much better than the PLS model calculated without the spectral smoothing (only 2nd derivative). Finally, the PLS model was used to predict the API concentration for the two industrial samples, withdrawn at the end of the blending operation of the manufacturing process. The residuals of the predicted concentration were –0.08% and 0.03% w/w, respectively, that represents an average relative error of prediction of 0.6% for a reference API concentration of 9% w/w. It has been demonstrated the need of spectral smoothing for the development of a PLS calibration model with an adequate predictive ability of industrial powder samples.

Conclusions

The two hand-held JDSU MicroNIR spectrometer versions have been used in different qualitative and quantitative quality control applications in the pharmaceutical industry.

Regarding counterfeit detection it has been proved that NIR spectroscopy can be used to rapidly distinguish fakes and illegal generics from the branded authentic products for tablets and capsule blends. NIR spectra can be achieved in seconds, ready to overlay in second derivative and export to multivariate software programs. The use of PCA can further help to visually discriminate the erectile dysfunction authentic and illegal generic brands, therefore providing a rapid methodology for screening at border control.

In another qualitative application, a spectral library for pharmaceutical raw material identification has been developed including 22 different compounds. Smoothing and second derivative has been applied as the spectral pretreatment. A correlation coefficient with a threshold of $r > 0.97$ has been used for positive identification. All the materials have been positively identified and only two pairs of components presented false positive identifications due to the high spectral similarity between them.

For quantitative applications, two examples of the determination of active principal ingredients in pharmaceutical powder samples have been presented. In both cases partial least squares (PLS) calibration models have been developed for the prediction of unknown test samples.

In the quantitative determination of the three crystalline active ingredients, acetylsalicylic acid, ascorbic acid and caffeine in blends with the two amorphous excipients cellulose and starch, competitive predictions comparable to results from previous benchtop and other portable instruments have been obtained. The evaluated concentration level was 14–26% (w/w) and a mean error of prediction of 0.8% (w/w).

The calibration and prediction errors obtained in the second application of a quantitative determination of an active ingredient in a pharmaceutical powder formulation also demonstrated, for a concentration range of 7–11% (w/w), an adequate predictive ability [0.2% (w/w) error of prediction].

In conclusion, JDSU's ultra-compact MicroNIR spectrometer enables rapid, non-destructive analysis of tablets, capsule blends and powder formulations. With a small footprint and ease of use, scientists and investigators can analyse samples in the field, on the road or in the testing laboratory.

Acknowledgements

Applied Chemometrics Research group are grateful to Spain's Ministry of Economy and Competitiveness for funding this research within the framework of Project CTQ2012-34392, also thanks to Laboratorios Menarini (Badalona, Spain) for kindly supplying samples, and Anna Palou and Jordi Cruz for the initial setup of the instrument. HWS thanks the Research Pool of the University of Duisburg-Essen for their long lasting support.

Table 9. Figures of merit of the PLS calibration models for the API determination.

	Calibration					Validation			
							Residuals t-test		
							t_{crit} = 2.365		
Spectral pre-treatment	Number of factors	% Y-explained variance	*RMSEC* (%w/w)	Correlation NIR vs REF	*RMSEP* (%w/w)	Correlation NIR vs REF	Residuals average	Residuals *SD*	t_{exp}
Smoothing Gaussian filter + SNV	1	74.624	0.553	0.864	0.799	0.631	−0.379	0.752	1.427
	2	87.264	0.392	0.934	0.705	0.700	−0.292	0.686	1.204
	3	96.109	0.216	0.980	0.578	0.858	−0.312	0.521	1.694
	4	97.573	0.171	0.988	0.588	0.833	−0.297	0.543	1.546
	5	98.504	0.134	0.992	0.580	0.846	−0.302	0.529	1.612
Smoothing Gaussian filter + SNV + 2nd derivative gap-segment	1	79.877	0.492	0.894	0.684	0.684	−0.194	0.701	0.782
	2	87.721	0.384	0.937	0.634	0.761	−0.239	0.627	1.077
	3	98.129	0.150	0.991	0.325	0.948	−0.145	0.310	1.324
	4	98.582	0.131	0.993	0.315	0.957	−0.156	0.292	1.511
	5	99.223	0.097	0.996	0.337	0.949	−0.168	0.312	1.518
1st derivative gap-segment	1	86.531	0.403	0.930	0.537	0.817	0.141	0.554	0.718
	2	92.557	0.299	0.962	0.415	0.889	0.036	0.441	0.227
	3	96.928	0.192	0.985	0.288	0.952	0.085	0.294	0.815
	4	98.086	0.152	0.990	0.241	0.966	0.037	0.254	0.406
	5	99.307	0.091	0.997	0.317	0.939	−0.067	0.331	0.573
Smoothing Gaussian filter + 1st derivative gap-segment	1	86.512	0.403	0.930	0.536	0.818	0.144	0.552	0.739
	2	92.463	0.301	0.962	0.417	0.888	0.037	0.443	0.238
	3	96.729	0.198	0.984	0.292	0.950	0.081	0.300	0.762
	4	97.854	0.161	0.989	0.245	0.964	0.029	0.260	0.316
	5	98.973	0.111	0.995	0.306	0.944	−0.070	0.318	0.618
2nd derivative gap-segment	1	84.693	0.429	0.920	0.538	0.822	0.171	0.546	0.886
	2	91.497	0.320	0.962	0.381	0.913	0.094	0.695	0.677
	3	95.046	0.244	0.975	0.321	0.958	0.178	0.286	1.764
	4	97.984	0.156	0.990	0.219	0.981	0.133	0.186	2.021
	5	98.418	0.138	0.992	0.222	0.983	0.147	0.178	2.342
Smoothing Gaussian filter + 2nd derivative gap-segment	1	84.595	0.431	0.920	0.535	0.825	0.172	0.542	0.895
	2	91.792	0.314	0.958	0.372	0.916	0.085	0.387	0.621
	3	95.007	0.245	0.975	0.312	0.958	0.162	0.285	1.612
	4	97.598	0.170	0.988	0.228	0.976	0.110	0.213	1.454
	5	98.347	0.141	0.992	0.230	0.984	0.122	0.175	1.962

The underlined rows are those with the best calibration performance and predictive ability.

References

1. E.W. Ciurczak and J.K. Drennen, *Pharmaceutical and Medical Applications of Near-Infrared Spectroscopy*. Marcel Dekker Inc., New York, USA (2002).
2. J. Luypaert, D.L. Massart and Y. Vander Heyden, "Near-infrared spectroscopy applications in pharmaceutical analysis", *Talanta* **72(3),** 865 (2006). doi: 10.1016/j.talanta.2006.12.023

3. Y. Roggo, P. Chalus, L. Maurer, C. Lema-Martinez, A. Edmond and N. Jent, "A review of near infrared spectroscopy and chemometrics in pharmaceutical technologies", *J. Pharm. Biomed. Anal.* **44,** 683 (2007). doi: 10.1016/j.jpba.2007.03.023

4. J. Mantanus, *New Pharmaceutical Applications Involving Near Infrared Spectroscopy as a PAT Compliant Process Analyzer*. PhD Thesis, University of Liege, Faculty of Medicine, Belgium (2012).

5. M.J. Lysaght, J.A. Van Zee and J.B. Callis, "Laptop chemistry: A fiber-optic, field-portable, near-infrared spectrometer", *Rev. Sci. Instrum.* **62,** 507 (1991). doi: 10.1063/1.1142095

6. T. Mackey and B. Liang, "The global counterfeit drug trade: Patient safety and public health risks", *J. Pharm. Sci.* **100(11),** 4571 (2011). doi: 10.1002/jps.22679

7. H. Wright and J. Nicholson, "Combating counterfeit medicines", *Pharm. J.* **282,** 193 (2009).

8. S.H.F. Scafi and C. Pasquini, *Analyst* **126,** 2218 (2001). doi: 10.1039/b106744n

9. M.J. Vredenbregt, D. Mooibroek, D. de Kaste and R. Hoogerbrugge, in *Near Infrared Spectroscopy: Proceedings of the 11th International Conference*, Ed by A.M.C. Davies and A. Garrido-Varo. NIR Publications, Chichester, UK, p. 1073 (2004).

10. M.J. Vredenbregt, D. Mooibroek and R. Hoogerbrugge, "Your Viagras—genuine, imitation, or counterfeit?", in *Handbook of Near-infrared Analysis*, Ed by D.A. Burns and E.W. Ciurczak. CRC, Boca Raton, USA, p. 631 (2008).

11. W.L. Yoon, R.D. Jee, G. Lee, A. Charvill and A.C. Moffat, "A non-destructive method to detect counterfeit medicines using near-infrared spectroscopy", *AAPS Pharm. Sci.* **3,** Supplement, Abstract 428 (2001).

12. S. Assi, R.A. Watt and A.C. Moffat, "Identification of counterfeit tablets and authentication of medicines in the international wholesaling supply chain using near infrared spectroscopy", in *Near Infrared Spectroscopy: Proceedings of the 14th International Conference*. IM Publications, Chichester, UK, p. 697 (2009).

13. M. Blanco and M.A. Romero, "Near-infrared libraries in the pharmaceutical industry: a solution for identity confirmation", *Analyst* **126,** 2212 (2001). doi: 10.1039/b105012p

14. M. Blanco, M. Bautista and M. Alcalà, "API determination by NIR spectroscopy across pharmaceutical production process", *AAPS PharmSciTech* **9(4),** 11305 (2008). doi: 10.1208/s12249-008-9156-3

15. H.A. Macleod, *Thin-Film Optical Filters*. CRC Press, Boca Raton, FL, USA, pp. 302–369, pp. 490–513 (2010).

16. D. Sorak, L. Herberholz, S. Iwascek, S. Altinpinar, F. Pfeifer and H.W. Siesler, "New developments and application of handheld Raman, mid-infrared and near-infrared spectrometers", *Appl. Spectrosc. Rev.* **47,** 83 (2012). doi: 10.1080/05704928.2011.625748